JOURNAL OF MATERIALS SCIENCE 35 (2000) 873–880

Physical, chemical and optical properties of aqueous L-arginine phosphate (LAP) solution

YONGKEE KIM
Pohang University of Science and Technology, Pohang Accelerator Laboratory/Linac Div., San 31 Hyojadong, Namgu, Pohang, Kyungbuk, 790-784, South Korea
E-mail: kimyk@postech.ac.kr

The mathematical modelling of the solution growth of high quality single crystals requires a good understanding of the fluid properties. In addition to the physical and mechanical properties a detailed knowledge of the optical parameters is required to study the dynamics of the crystal growth process. Measurements of polarizability, refractive index, optical dispersion, solubility, pH, viscosity, and density were performed on aqueous L-Arginine phosphate (LAP) solutions. The index of refraction was measured with an Abbe refractometer at four different wavelengths. Optical dispersion was calculated using the Cauchy's equation. Effects of the density and kinematic viscosity of the LAP solution are discussed in terms of the dimensionless Grashof and Reynolds number allowing a better understanding of the benefits of operating under the 'micro-g' conditions of space for the solution growth of single crystals. The Cauchy's formula and Sellmeier formula of the refractive index have been used to determine both the gradients dn/dc and dn/dT as a function of wavelength and the polarizability of the LAP solution. The polarizability of the LAP crystal, α_2, was found to be 14.50 cm^3/mol and this value was in good agreement with experimental data obtained and analyzed using the well-known Lorentz-Lorenz formula.

1. Introduction

Crystals are taking a primary part in areas of modern technology involving e.g. lasers, sensors, interferometers, memory chips, detectors, electrical devices, and optical components. Frequency conversion is one of the important and popular techniques to extend the useful wavelength range of laboratory lasers. Over three decades there have been extensive efforts to develop new materials. Despite these efforts, only a handful of nonlinear crystals are commonly available for frequency conversion. These crystals are lithium triborate (LiB_3O_5 known as LBO), magnesium-oxide-doped lithium niobate ($MgO:LiNbO_3$), potassium niobate ($KNbO_3$), barium borate (BaB_2O_4, commonly referred to as BBO), potassium titanyl phosphate ($KTiOPO_4$ known as KTP), and potassium dihydrogen phosphate (KH_2PO_4 known as KDP).

The NOVA laser facility at Lawrence Livermore National Laboratory currently uses 74-cm aperture segmented arrays of potassium dihydrogen phosphate (KDP) for laser fusion experiments [1]. The group of KDP materials remains the most widely used crystals for frequency conversion [2]. The key factors for material selection depend not only upon the laser conditions—beam size, beam quality and beam power density—but also upon the crystal's physical properties, such as, transparency, damage threshold, conversion efficiency, phase matching, and temperature stability. L-Arginine Phosphate monohydrate, $(H_2N)_2{}^+CNH(CH_2)_3CH(NH_3)^+COO^-H_2PO_4{}^-H_2O$, abbreviated as LAP, is a more recent nonlinear optical (NLO) material first introduced by Chinese material scientists in 1983 [3]. An attractive feature of LAP is in its direct replacement for KDP in a wide range of devices. This is because LAP crystals are phase matchable for all nonlinear processes where KDP is also phase matchable, and because they benefit from a substantially higher efficiency than KDP [2]. Also it is less hygroscopic and easier to handle than KDP, and large crystals can be grown with relative ease [4]. LAP and KDP crystals are usually grown from aqueous solution by a temperature lowering technique. Growth of crystals from aqueous solutions is one of the standard and important techniques in the optical industry involving the production of large crystals.

After the discovery of LAP, this crystal caught the attention of many research workers because of its high nonlinearity, wide transmission ranges (220 nm–1950 nm), high conversion efficiency ($\eta = 38.9\%$), and high damage threshold [5–8]. The damage threshold of the LAP (>30 J/cm^2) was found to be about twice as high as for the best quality commercially available KDP [2, 4]. The crystal structure of LAP has been reported extensively by Aoki *et al.*, [6]. Fig. 1 shows the structure of LAP along the *c*-axis [6]. Oxygen atoms are indicated by double circles, nitrogen atoms by shaded circles and carbon atoms by single circles. Water molecules are labeled *W*. Hydrogen bonds are

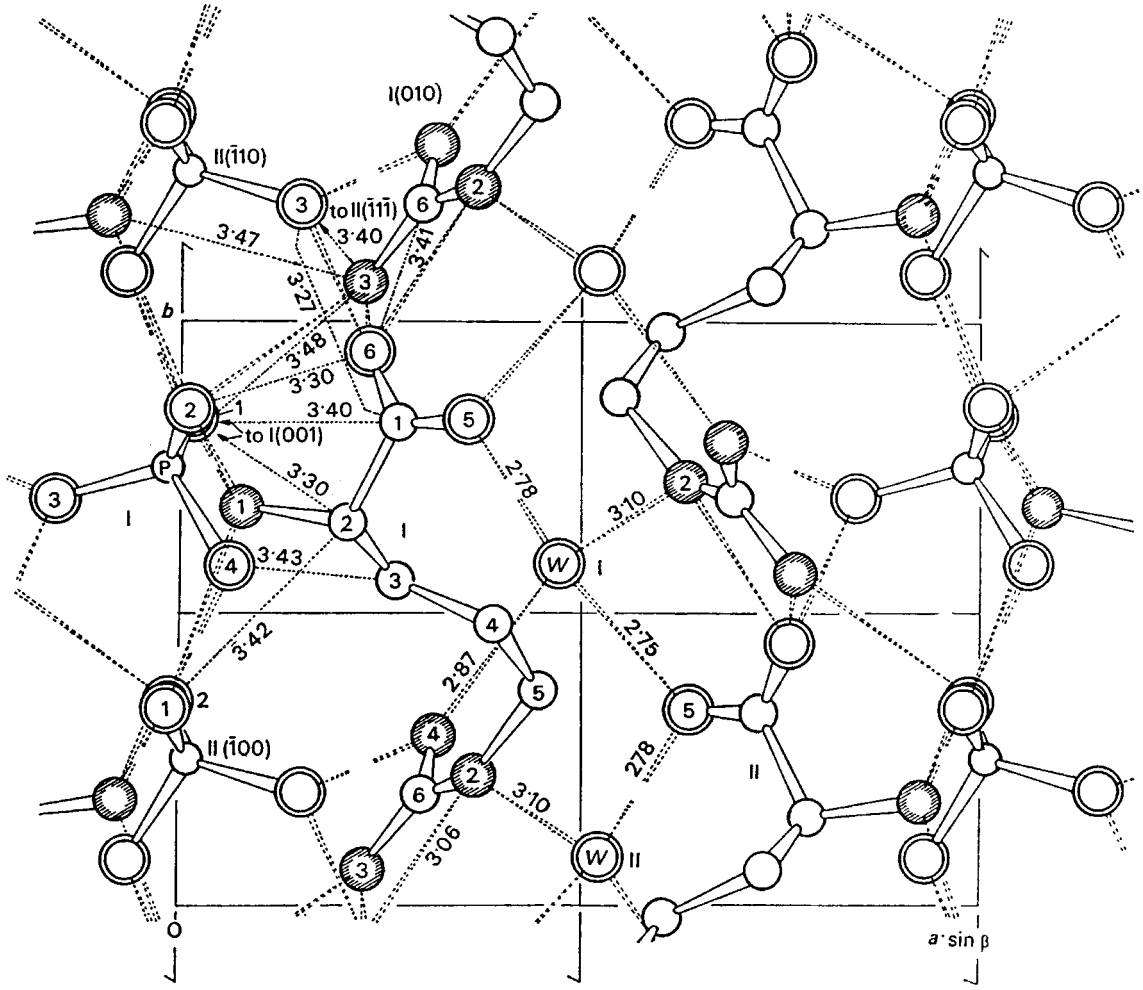

Figure 1 The crystal structure of the LAP along the *c*-axis. Oxygen atoms are indicated by double circles, nitrogen atoms by shaded circles and carbon atoms by single circles. Water molecules are labeled *W*. Hydrogen bonds are shown by double broken lines (adapted from [6]).

shown by double broken lines. The crystal structure consists of alternate layers of phosphate groups and arginine molecules stacked along the *a*-axis and held together by hydrogen bonds. The space group of LAP crystal is $P2_1$, with the twofold axis parallel to the *b*-axis by convention. The unit cell parameters of LAP crystal are $a = 10.85$ Å, $b = 7.91$ Å, $c = 7.32$ Å with $\beta = 98.0^\circ$ where β is the angle between *a* and *c* axes, and *b* is the two fold axis [6]. Some of the important properties of the LAP crystal are summarized in Table I. Several papers have been published for the growth of LAP crystals using similar growth conditions [7, 8]. The growth of LAP with sulphate (LAPS) and its structural, mechanical, electrical and optical properties have also been reported [9]. All these papers, however, have only reported on the growth and properties of LAP crystals. A better understanding of crystal growth dynamics in aqueous solution requires a knowledge of the physical, chemical, and optical properties of aqueous LAP solutions. This will allow better modeling of the crystal growth and is particularly important for crystal growth in the 'micro-g' conditions of space. Unfortunately, many basic physical and optical properties of the aqueous LAP solution have hitherto not been measured. This paper reports upon the physical, chemical and optical properties of the aqueous LAP solution and their dependence on temperature, concentration, and wavelength for the growth of good optical quality single LAP crystals. This information will allow a better understanding of the growth dynamics from a supersaturated solution. The measurements performed include polarizability, refractive index, optical dispersion, solubility, pH, viscosity, and density of aqueous LAP solutions.

2. Physical properties of LAP solution

LAP crystalline powder is not commercially available to date. Thus, the LAP powder was synthesized in the laboratory by dissolving 255 g of L-arginine and 78 g of phosphoric acid in 700 ml of deionized water at 50°C. This solution was heated while stirring for 2 hours for full chemical reactions. This fully reacted solution was filtered 5 times with membrane filters. By evaporating this filtered solution, the crystallized LAP powder was obtained. This powder was further purified by a recrystallization process in deionized water. For the measurement of various properties of the aqueous LAP solution this recrystallized LAP powder was used throughout this works.

2.1. Solubility

An investigation of solubility is a pre-requisite of crystal growth especially from solution. The solubility of

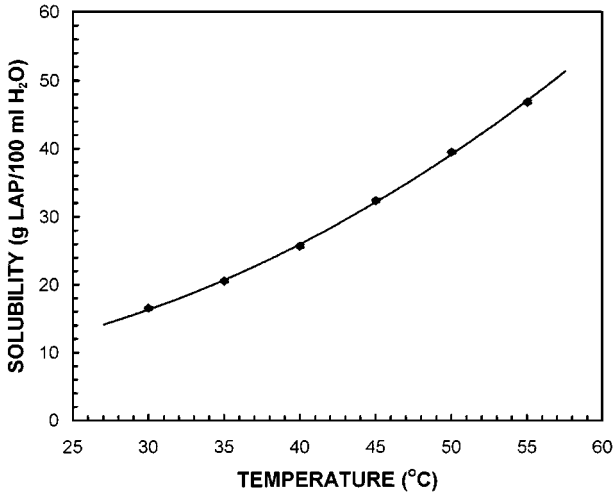

Figure 2 The solubility curve of the aqueous LAP solution.

the LAP was determined in deionized water using a double-walled temperature jacket cell. 50 ml of deionized water was poured into the cell, and its temperature maintained constant at a desired temperature to an accuracy of $\pm 0.01^{\circ}$C by circulating water through the outer part of the cell. This double-walled cell was placed on a magnetic stirrer. Initially at a given temperature 1 g of LAP powder (weighed by Mettler H54AR balance with an accuracy of ± 0.001 g) was added to the 50 ml of water and its solubility observed whilst constantly stirring. The procedure of adding LAP powder into the solvent was repeated, reducing the amount of LAP as the saturation point was judged to be reached. Towards the end only 0.05 g of LAP powder was added until a small amount of LAP was left undissolved in the solution. This was then repeated for other temperatures. The solubility curve of the LAP from 30°C to 55°C is shown in Fig. 2 at pH of 4.3. The saturated LAP solutions have a pH values of 4.2–4.3. This pH can be increased by adding L-Arginine to the LAP solution. It was observed that increasing of pH value increases the solubility of LAP.

2.2. Density

The density of a saturated LAP solution was measured using a chain balance and glass specific gravity plummet capable of a resolution of ± 0.0001 g/ml. The apparatus was calibrated with deionized water prior to the measurement of the LAP solution. The results of the calibration with deionized water were confirmed using the data available in handbook of chemistry and physics. Density measurements were made from 30°C to 40°C and could not go over 40°C because of the maximum working temperature of the densitometer. The results of density measurements obtained were: (a) 1.0495 g/ml at 30°C (b) 1.0104 g/ml at 35°C (c) 1.0038 g/ml at 40°C. There are basically two mechanisms involved in density gradients around a growing crystal in solution. First, the density gradient results from temperature variations. The values of the density were dependent on the fluid temperature. Thus the density gradients caused by temperature variations in the fluid. This temperature variations of the fluid induce convection forces that the solution to flow upward and generates significant variations in concentrations in different parts of the fluid. Second, the density gradient results from solute depletion. Convection in solution growth is also caused by density gradients that occur when solute is depleted from the solution at the growing crystal surfaces [10]. Effects of density-driven convection greatly affect the growth rate of the crystals with upward motions of the solutions (*i.e.* buoyancy forces). This buoyancy-driven flow occurred in the form of a plume and was well illustrated in Fig. 2. of reference [11], Fig. 1. of reference [13], and Fig. 4. of reference [14]. These figures also show that a buoyancy force induces a vertical motion of the fluid where ascending warm solution from the bottom of the growing crystal is replaced by inflow of cooler solution. Observations were made that the density of the LAP solution depends on temperature, generally decreasing with increasing temperature due to expansion of solution.

2.3. Viscosity

Kinematic viscosity values of the aqueous LAP solution for different temperatures were measured with a viscometer (Ubbelohde) tube immersed in a controlled temperature water bath. The device was calibrated with deionized water at several different temperatures before the real measurements on LAP. The kinematic viscosity was determined by measuring the time required to draw a known volume of fluid through a capillary with a constant pressure difference across the fluid column. The results of viscosity measurements of the saturated LAP solutions at pH 4.3 over a temperature range of 30°C to 55°C are plotted as a function of temperature in Fig. 3. Note that the viscosity decreases slightly as the temperature is increased up to 35°C, and start to increase as the temperature is increased further from 35°C to 45°C.

The importance of viscosity for crystal growth can be examined from the dimensionless Grashof number, G_r, which governs convection of the fluid and is given by [12]

$$G_r = \frac{g\beta\Delta TL^3}{\nu^2}, \tag{1}$$

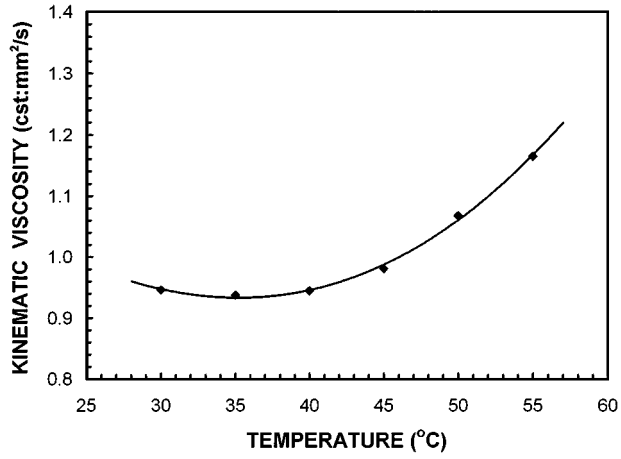

Figure 3 The kinematic viscosity of the saturated LAP solution as a function of temperature.

where, g is gravitational field, β the thermal expansion coefficient, ΔT the temperature difference, L the size of the cell (m), and ν the kinematic viscosity of the fluid. This Grashof number indicates the ratio of the buoyancy force to viscous force acting on the fluid. Its role in free convection is much the same as that of the Reynolds number in forced convection. The advantage of growing crystals in space is seen from the Grashof number since the grows effects of earth growing (g effect) are nearly removed and the density-driven convective flow almost eliminated. The Grashof number G_r plays the same role in free convection that the Reynolds number plays in forced convection.

The Reynolds number R_e is defined as follows

$$R_e \equiv \frac{VL}{\nu} = \frac{\rho VL}{\mu}, \tag{2}$$

where V is velocity (m/s), L is characteristic length (m), ν is kinematic viscosity (m^2/s), ρ is density, and μ is viscosity (kg/s·m). The Reynolds number R_e provides a measure of the ratio of the inertial to viscous forces acting on a fluid element. Other than this Grashof number G_r and Reynolds number R_e, several important dimensionless numbers, i.e., Schmidt number S_c, Prandtl number P_r, are also closely related with viscosity value of the fluid. These dimensionless numbers play a key role in heat transfer and mass transfer of the fluid for crystal growth. In solution crystal growth, the fluid motion is associated with the moving of large numbers of molecules collectively or as aggregates. This fluid motion contributes to heat transfer in the presence of a temperature gradient. The flow patterns may generate significant variations in concentration at different part of crystal, thus leading to non-uniform growth rate [14].

A temperature gradient constitutes the driving potential for heat transfer. Similarly, concentration gradient of a species in a mixture (or solution) provides the driving potential of mass transfer. Both conduction heat transfer and mass diffusion are transport processes that originate from molecular activities. As crystal growers we are actually concerned with two aspects of the nutrient-to-crystal transport: (a) With the mass flux across an interface, which we will call the interfacial flux and determines the crystal growth rate; and (b) With the concentration profile of growth species in the nutrient adjacent to the crystal, which is an essential parameter in describing morphological stability.

3. Optical properties of LAP solution and crystal

A detailed knowledge of the optical parameters is required to study the dynamics of the crystal growth process using optical techniques such as interferometry, ellipsometry, and holography. Most optical parameters are closely related to temperature, and concentration change as well as density change. The index of refraction is one of the most important parameters for transparent materials in the study of growth dynamics and growth modelling. The well-known effect of refractive index is its dependence on wavelength, concentration, and temperature. The value of refractive index is also closely related to the atomic structure of the material.

3.1. Refractive index of LAP solution

The index of refraction of the aqueous LAP solution of a known concentration was measured. The measurements were carried out using an Abbe refractometer at four different wavelengths at 30°C using a temperature controlled sample stage. The values of refractive index measurements on the aqueous LAP solution were; (a) 1.3631 at 479.99 nm, (b) 1.3597 at 546.07 nm, (c) 1.3580 at 589.30 nm, (d) 1.3562 at 643.85 nm. The Cauchy's dispersion formula is a useful tool for the determination of refractive indices at other wavelengths. The Cauchy's formula of refractive index as a function of wavelength (λ) is given by

$$n(\lambda) = A + \frac{B}{\lambda^2} + \frac{C}{\lambda^4}, \tag{3}$$

where A, B, and C are constants which depend on the particular characteristics of the sample and λ is the wavelength (in nanometers). If refractive indices at three wavelengths are known, the constants A, B, and C can be obtained from Equation 3. The values of three constants are $A = 1.34537905$, $B = 4998.594721$, and $C = -212597275$ for the aqueous LAP solution at 30°C. With these three constants (A, B, and C) determined accurately, good values of refractive index can be obtained over all wavelength from absorption bands. The plot of refractive index of the aqueous LAP solution as a function of wavelength is shown in Fig. 4. The dispersion curve is just the differential of Equation 3, that is $dn/d\lambda = -2B/\lambda^3 - 4C/\lambda^5$. For the aqueous LAP solution, the dispersion can be expressed as follows by substituting for the constants B and C,

$$\frac{dn}{d\lambda} = -\frac{9997.189442}{\lambda^3} + \frac{850389100}{\lambda^5}. \tag{4}$$

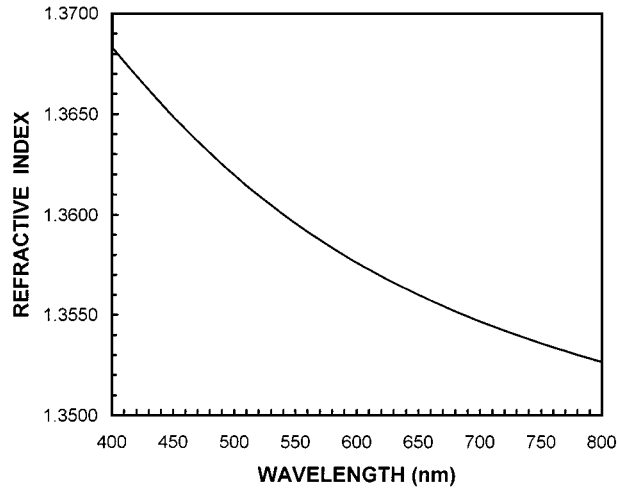

Figure 4 The refractive index of the aqueous LAP solution as a function of wavelength by the Cauchy's formula.

3.2. Gradient dn/dc

The refractive index variation as a function of concentration is another important parameter for the study of crystal growth dynamics in aqueous solution. For the determination of the concentration gradient of the solution, the Lorentz-Lorenz equation was used from which the relationship dn/dc was obtained at different wavelengths. From the Lorentz-Lorenz equation the specific refractivity $\bar{r}$ can be defined and is given by

$$\frac{n^2-1}{\rho(n^2+2)} = \bar{r}, \tag{5}$$

where ρ is the density. Note that $\bar{r}$ is a function of the wavelength of light. By differentiating Equation 5 with respect to ρ, one obtains

$$\frac{\mathrm{d}n}{\mathrm{d}\rho} = \frac{(n^2-1)(n^2+2)}{6n\rho}. \tag{6}$$

In typical solution crystal growth experiments, concentration changes are proportional to density changes. Figure 7 of Kroes' paper [11] clearly shows the validity of this assumption. Concentration and density are independent of wavelength. Thus, when concentration or density remains fixed, Equation 6 can be rewritten as follows

$$\frac{\mathrm{d}n}{\mathrm{d}c} \propto \frac{(n^2-1)(n^2+2)}{n}. \tag{7}$$

Therefore, if dn/dc at one n (or λ) is known, it can easily be determined at other wavelengths. The gradient dn/dc can be written as $\Delta n/\Delta c$ where Δn $(= n_2 - n_1)$ is the refractive index change (or difference) on going from a saturated solution at one temperature to another, and Δc is the corresponding concentration difference (= solubility difference of the LAP powder in one liter of H_2O). Therefore the gradient dn/dc of a LAP solution can be obtained by knowing the solubility of LAP and the variation of the refractive index of LAP solutions at various temperatures. Fig. 5 shows the variation of the refractive index with temperature and concentration of the LAP solution at 589.3 nm measured using an Abbe refractometer at eight different temperatures from 25°C to 50°C with temperature controlled sample stage. The Δn of the saturated LAP solution is 0.0038 from the refractive index variation curve of Fig. 5, and Δc is 40.2 [g LAP/liter H_2O] from the solubility curve shown in Fig. 2, as the saturation temperature changes from 35°C to 30°C. Thus the gradient dn/dc can be determined over this temperature range. The value of the gradient dn/dc for the LAP solution is 0.000094527 [g LAP/liter H_2O]$^{-1}$ at 589.3 nm. By substituting this value of dn/dc into the left hand side of the Equation 7, the proportionality constant 3.9557×10^{-5} was determined. The final result of the gradient dn/dc between the temperature range 30°C and 35°C is as follows

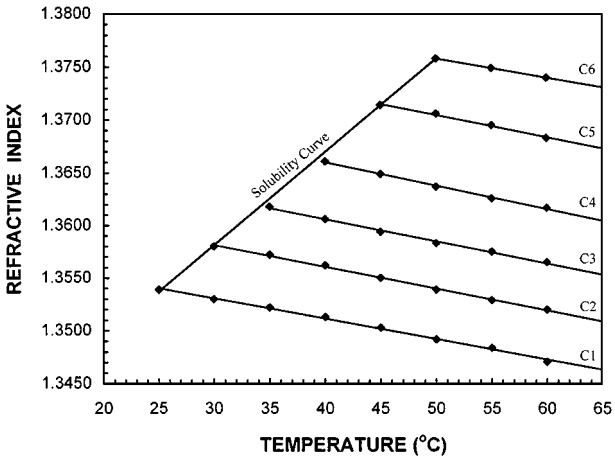

Figure 5 Variation of the refractive index with temperature and concentration of the LAP solution at 589.3 nm measured using an Abbe refractometer. (C1, C2, C3, C4, C5, and C6 are the concentrations of the LAP at 25°C, 30°C, 35°C, 40°C, 45°C, and 50°C respectively).

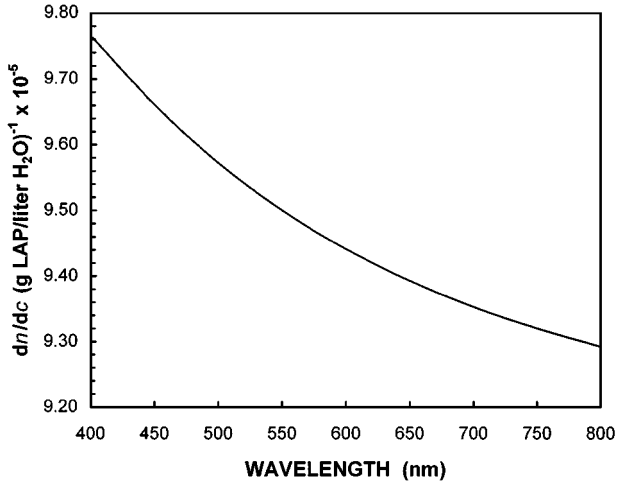

Figure 6 A plot of gradient dn/dc of the LAP solution as a function of wavelength.

$$\frac{\mathrm{d}n}{\mathrm{d}c} = 3.9557 \times 10^{-5} \times \frac{(n^2-1)(n^2+2)}{n}[\text{g LAP/liter } H_2O]^{-1} \tag{8}$$

Fig. 6 represents a plot of the gradient dn/dc between the temperature range 30°C and 35°C. Similarly, Equations 3 and 7 can be combined to obtain the concentration gradient dn/dc at other temperature ranges and different wavelengths.

3.3. Gradient dn/dT

For the solution growth of crystal, temperature variations play an important role particularly when mass and heat transfer processes occur. The refractive index variations as a function of temperature T and concentration c are two important functions in the analysis of interference fringes [15–20]. Detailed interference techniques are explained in reference 15 through 20 for each of their techniques. Interferometry techniques are very sensitive, accurate and powerful tools for the determination of optical parameters of solids, gases, and liquids and also have been used in sensors, detectors, fiber optics, communications, and many industrial applications. With these techniques, the difference of optical

path length is measured between the reference beam and the beam reflected from the medium. These two beams produce an interference pattern from where the desired informations and parameters can be obtained.

Figure 4 of Kroes' paper [11] shows that at a given wavelength, the gradient dn/dc and dn/dT are practically constant for typical temperature and concentration ranges of interest. The procedure used to determine the temperature gradient dn/dT involved using the relationship determined by Murphy and Alpert [21] as follows

$$\frac{dn}{dT} = -\frac{3n(n^2-1)\beta}{2(2n^2+1)} \tag{9}$$

where β is the coefficient of the thermal expansivity of the liquid and is independent of wavelength. At this stage it is worth mentioning the desired concentrations and temperatures relevant in fluid analysis are explicitly independent. Thus, the partial and total derivatives are equivalent. The relationship of Equation 9 gives the values of dn/dT accurately to within ~2% [18]. Thus, if n and dn/dT at one wavelength are known, we can determine the constant β from Equation 9. The refractive index of the LAP solution at 30°C was 1.3580 and 1.3572 at 35°C for a given constant concentration as shown in Fig. 5 for measurements made at 589.3 nm. Thus the Δn of the saturated LAP solution is 0.0008 for a given concentration, and ΔT is −5°C. Therefore, the gradient dn/dT at 589.3 nm has a value of $-0.00016°C^{-1}$. By substituting this value into the left hand side of the Equation 9, β can be obtained and used in the right hand side of Equation 9 to give the following result:

$$\frac{dn}{dT} = -6.3074 \times 10^{-4} \times \frac{n(n^2-1)}{2n^2+1} \,°C^{-1}. \tag{10}$$

Since β is considered constant with wavelength, substituting values of refractive index at different wavelength allows dn/dT to be determined as a function of wavelength. This is shown in Fig. 7.

3.4. Polarizability and refractive index of LAP crystals

The refractive indices of a LAP crystal can be determined at room temperature by using the Sellmeier formula:

$$n^2 = A + \frac{B}{\lambda^2 + C} + D\lambda^2, \tag{11}$$

where λ is the wavelength in microns, and A, B, C, and D are constants. The Sellmeier formula for a LAP crystal for each dielectric axis (λ, β, and γ) is given by [22]

$$n_\alpha^2 = 2.2439 + \frac{0.0117}{\lambda^2 - 0.0179} - 0.0111\lambda^2, \tag{12}$$

$$n_\beta^2 = 2.4400 + \frac{0.0158}{\lambda^2 - 0.0191} - 0.0212\lambda^2, \tag{13}$$

$$n_\gamma^2 = 2.4590 + \frac{0.0177}{\lambda^2 - 0.0226} - 0.0162\lambda^2, \tag{14}$$

The refractive indices of the LAP crystal at 25°C are plotted in Fig. 8 as a function of wavelength.

The polarizability of the LAP crystal and the refractive index of an aqueous solution can be confirmed by the well-known Lorentz-Lorenz formula

$$\frac{n^2-1}{n^2+2} = \frac{4\pi}{3}(\alpha_1 N_1 + \alpha_2 N_2), \tag{15}$$

where n is the refractive index of the solution, α_1 and α_2 are the polarizability of H_2O and LAP, respectively, N_1 and N_2 are the moles of H_2O and LAP in the solution. The refractive index of the saturated LAP solution at 30°C was 1.3565 at 633 nm from the Cauchy's formula Equation 3. The left hand side of Equation 15 is then $(n^2-1)/(n^2+2) = 0.2187$.

The value of the polarizability of H_2O, α_1, has been reported by Ogawa [23], Hirano [24], and Mantani [25] giving the value of 0.886 cm^3/mol. Their agreement of α_1 was less than 1% error range. The polarizability of LAP crystal, α_2, was found to be 14.50 cm^3/mol and

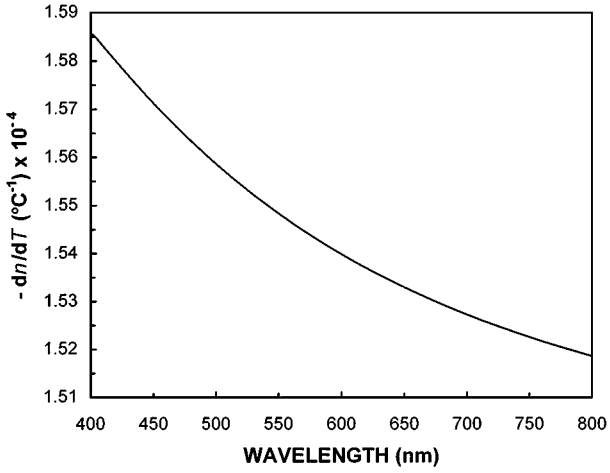

Figure 7 A plot of temperature gradient dn/dT of the LAP solution as a function of wavelength.

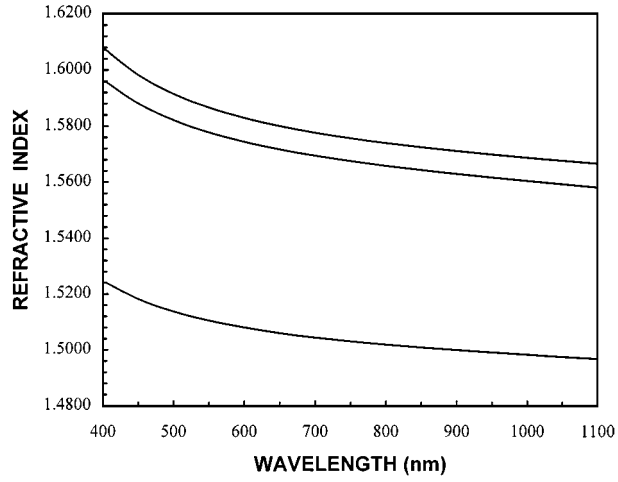

Figure 8 The refractive indices of the LAP crystal at 25°C as a function of wavelength by the Sellmeier formula.

TABLE I Physical and opticla properties of the LAP crystal (some numbers are adapted from the *Laser and Optronics*, November1987)

L-arginine phosphate (LAP)	Values
Crystal structure	Monoclinic
Space group	$P2_1$
Formula weight	290.1 g
Unit cell parameters	$a = 10.85$ Å, $b = 7.91$ Å, $c = 7.32$ Å
Unit volume	621.9 Å^3
β (the angle between the a and c axes)	$\beta = 98.0^\circ$
Transmission wavelength	220 nm–1950 nm
Conversion efficiency η	38.9% (532 nm–266 nm)
Damage threshold	
at 1064 nm	10 GW/cm^2 (with 1 ns pulse width)
at 526 nm	60 GW/cm^2 (with 0.6 ns pulse width)
Refractive indices	
at 1064 nm	$n_\alpha = 1.4974$, $n_\beta = 1.5598$, $n_\gamma = 1.5376$
at 532 nm	$n_\alpha = 1.5114$, $n_\beta = 1.5794$, $n_\gamma = 1.5883$
Density	1.531 g/cm^3
Thermal conductivity coefficient	0.59 W/m K
Melting point	~130°C
Phase-matching range	440–1950 nm
Vicker hardness	
plane (100)	240 kg/mm^2
plane (010)	154 kg/mm^2

was obtained by using the averaged value of the refractive indices of LAP crystal at 633 nm: $(n_\alpha + n_\beta + n_\gamma)/3 = (1.5067 + 1.5725 + 1.5809)/3 = 1.5534$ and the corresponding density is 1.531 g/cm^3 (see Table I). A saturated LAP solution at 30°C was made by dissolving 165 g of crystalline LAP powder into 1000 g of deionized and distilled water. The density was 1.0495 g/cm^3. The molar weight of the LAP crystal is 290.1 g and that of water is 18 g. From this information, the saturated LAP solution contains an $N_1 = 0.05$ mol/cm^3 of H_2O, and an $N_2 = 5.13 \times 10^{-4}$ mol/cm^3 of LAP. Substituting all the obtained values of α and N into the right hand side of Equation 15 gives 0.2166 which is in good agreement with the calculated value 0.2187 in the left hand side of Equation 15. The small difference of 0.0021 (≈1%) between the left and right hand side of Equation 15 comes mainly from the use of an averaged refractive index value for LAP crystals and the experimental errors on measurements of solubility and density. The good agreement obtained justifies the use of the Lorentz-Lorenz equation in the entire part of this works.

4. Summary

The growth and perfection of crystals from the aqueous solution phase is important both from the fundamental and application interests. To this end, an extensive study has been made on the physical, chemical and optical properties of aqueous LAP solutions to allow the modelling and hence a better understanding of the conditions to produce good quality LAP crystals. However the data obtained in this works has not yet been used to grow much better crystals. This work is actually ongoing and will be applied for the growth of better crystals later on. The solubility of LAP was determined over the temperature range of 30°C to 55°C at a pH of 4.3 in deionized water using a double-walled cell. The saturated LAP solutions had a pH value of 4.2–4.3.

The results of the LAP solution density measurements were: (a) 1.0495 g/ml at 30°C (b) 1.0104 g/ml at 35°C (c) 1.0038 g/ml at 40°C. The values of the density were dependent on the fluid temperature and the buoyancy-driven convection resulting from the fluid density gradients caused by temperature variations in the fluid. Convection in solution growth is caused by density gradients that occur when solute is depleted from the solution at the growing crystal surfaces. The viscosity values of the saturated LAP solutions were made at pH 4.3 over a temperature range of 30°C to 55°C. The viscosity was found to decrease slightly at first as the temperature was increased to 35 °C, and then to rise again as the temperature was increased from 35°C to 55°C.

The index of refraction of an aqueous LAP solution of a known concentration was measured at various wavelengths. The values of refractive indices were; (a) 1.3631 at 479.99 nm, (b) 1.3597 at 546.07 nm, (c) 1.3580 at 589.30 nm, (d) 1.3562 at 643.85 nm. The refractive indices of the LAP solution (400–800 nm) were determined using the Cauchy's dispersion formula. The measurements of refractive index data in four different wavelengths will be extremely useful for the surface studies of the LAP crystals using an ellipsometry.

For the solution growth of crystal, concentration and temperature plays an important role in mass and heat transfer. The refractive index variations versus temperature T and concentration c are two important parameters for the analysis of interference fringes. The gradient dn/dc of the LAP solution was determined as: $dn/dc = 3.9557 \times 10^{-5} \times (n^2 - 1)(n^2 + 2)/n$ [g LAP/liter H_2O]$^{-1}$ at 589.3 nm and used to obtain the gradients dn/dc at different wavelengths from Equations 3 and 7. The temperature gradient dn/dT of the LAP solution was found to be $dn/dT = -6.3074 \times 10^{-4} \times n(n^2 - 1)/2n^2 + 1°C^{-1}$ at 589.3 nm and again used to determine the dn/dT at different wavelengths. In solution growth, the fluid motion contributes to heat transfer in the presence of a temperature gradient. The flow patterns may generate significant variations in concentration at different parts of the crystal, thus leading to a non-uniform growth rate. A temperature gradient constitutes the driving potential for heat transfer. Similarly, a concentration gradient of a species in a mixture (or solution) provides the driving potential for mass transfer. Both conduction heat transfer and mass diffusion are transport processes that originate from molecular activities.

The polarizability of the LAP crystal, α_2, was found to be 14.50 cm^3/mol and this value is confirmed by the well-known Lorentz-Lorenz formula using the measured refractive index values of the LAP solution.

Acknowledgements

The author would like to thank Pohang University of Science and Technology and Pohang Accelerator Laboratory for giving me a support to publish this paper. Many thanks goes to Dr. B. B. Lal for reading thoroughly the manuscript, and Dr. T. G. George, Dr. B. R. Reddy for their useful suggestions and comments throughout this work, and Thomas Glasgow NASA Lewis Research Center for the support of this work through a research grant NAG3-1429.

References

1. M. A. SUMMERS, J. D. WILLIAMS, B. C. JOHNSON and D. EIMERL, *Proc. Soc. Photo-Opt. Instrum. Eng.* **622** (1986) 161.
2. D. EIMERL, S. VELSKO, L. DAVIS, F. WANG, G. LOIACONO and G. KENNEDY, *IEEE J. Quantum Electronics* **25** (1989) 179.
3. D. XU, M. JIANG and Z. TAN, *Acta Chim. Sinica.* **41** (1983) 570.
4. P. V. KOLINSKY, *Opt. Eng.* **31** (1992) 1676.
5. J. T. LIN and C. CHEN, *Laser Optronics* **Nov.** (1987) 59.
6. K. AOKI, K. NAGANO and Y. IITAKA, *Acta Cryst.* **27** (1971) 11.
7. S. B. MONACO, L. E. DAVIS, S. P. VELSKO, F. T. WANG and D. EIMERL, *J. Crystal Growth* **85** (1987) 252.
8. T. KOBAYASHI (ed.), in "Nonlinear Optics of Organics and Semiconductors, Proc. Intern. Symp., Tokyo, 1988," Springer Proceedings in Physics, Vol. 36 (Springer, Berlin, 1989) p. 206.
9. G. RAVI, K. SRINIVASAN, S. ANBUKUMAR and P. ROMASAMY, *J. Crystal Growth* **137** (1994) 598.
10. L. J. DELUCAS *et al.*, *ibid.* **76** (1986) 681.
11. R. L. KROES and D. REISS, *ibid.* **69** (1984) 414.
12. H. D. YOO, W. R. WILCOX, R. LAL and J. D. TROLINGER, *ibid.* **92** (1988) 101.
13. P. T. SHLICHTA, *ibid.* **76** (1986) 656.
14. M. L. PUSEY, *ibid.* **122** (1992) 1.
15. F. MAYINGER and W. PANKNIN, in "Holographic Two-Wavelengths Interferometry for Measurement of Combined Heat and Mass Transfer, in Combustion Measurements: Modern Techniques and Instrumentation," edited by R. Goulard (Academic, New York, 1976) p. 270.
16. A. ECKER, *J. Thermophys. Heat Transf.* **2** (1988) 193.
17. A. ECKER, D. O. FRAZER and J. I. D. ALEXANDER, *Metall. Trans.* A **20** (1989) 2517.
18. C. S. VIKRAM, H. J. CAULFIELD, G. L. WORKMAN, J. D. TROLINGER, C. P. WOOD, R. L. CLARK, A. D. KATHMAN and R. M. RUGGIERIO, in "Two-color Holography Concept (T-CHI), Final Technique Report," Contract No. NAS8-38078, NASA Marshall Space Flight Center, Huntsville, Alabama, 1990, p. 6.
19. J. M. MEHTA, *Appl. Opt.* **29** (1990) 1924.
20. C. S. VIKRAM and W. K. WITHEROW, *Exp. Mechanism.* **32** (1992) 74.
21. C. G. MURPHY and S. S. ALPERT, *Amer. J. Phys.* **39** (1971) 834.
22. V. G. DMITRIEV, G. G. GURZADYAN and D. N. NIKOGOSYAN, in "Handbook of Nonlinear Optical Crystals," 2nd ed. (Springer-Verlag, Heidelberg, 1997) p. 245.
23. T. OGAWA and K. SATOH, *J. Chemical and Engineering Data* **21** (1976) 33.
24. E. HIRANO and T. OGAWA, *J. Crystal Growth* **51** (1981) 113.
25. M. MANTANI, M. SUGIYAMA and T. OGAWA, *ibid.* **114** (1991) 71.

Received 9 February
and accepted 12 July 1999